

HI 21 cm absorption in low z damped Lyman- α systems

Nissim Kanekar *, Jayaram N Chengalur **

National Centre for Radio Astrophysics, Post Bag 3, Ganeshkhind, Pune 411 007

Received mmddyy/ accepted mmddyy

Abstract. We report Giant Metrewave Radio Telescope (GMRT) 21 cm observations of two confirmed and one candidate low redshift damped Lyman- α systems (DLAS). HI absorption was detected in the two confirmed systems, at $z = 0.2378$ and $z = 0.5247$, with spin temperatures of 2050 ± 200 K and 330 ± 70 K respectively. The non-detection of absorption in the third (candidate) system places an upper limit on its optical depth, which in turn implies a 3σ lower limit of 850 K on its spin temperature. Ground based K-band imaging observations (Turnshek et al. 2000) have identified the low T_s absorber with a spiral galaxy while the high T_s system appears to be an LSB galaxy. This continues the trend noted earlier by Chengalur & Kanekar (2000) of low spin temperatures for DLAS associated with spiral galaxies and high spin temperatures for those with no such association.

Combining these new results with 21 cm observations from the published literature, we find that (1) The 21 cm equivalent width (EW_{21}) of DLAS increases with increasing N_{HI} . Further, absorbers associated with spiral galaxies have systematically higher EW_{21} at the same N_{HI} than DLAS with no such association, (2) DLAS at high redshift ($z \gtrsim 2$) have small velocity spreads ΔV , while, at low redshift ($z \lesssim 2$), both large and small ΔV are observed. These trends are in qualitative agreement with hierarchical models of galaxy formation.

Key words: galaxies: evolution: – galaxies: formation: – galaxies: ISM – cosmology: observations – radio lines: galaxies

1. Introduction

Damped Lyman- α systems (DLAS), are the rare, high HI column density ($N_{\text{HI}} \gtrsim 10^{20} \text{ cm}^{-2}$) absorbers seen in spectra taken against distant quasars. These systems are the major observed repository of neutral gas at high redshift

($z \sim 3$) and are thus logical candidates for the precursors of modern-day spiral galaxies (Wolfe 1988). However, despite more than a decade of systematic study, the structure and evolution of the absorbers remains an issue of much controversy. The original optical surveys to detect DLAS were carried out with the prime motivation of detecting disk galaxies at high redshift (e.g. Wolfe et al. 1986). Follow-up observations of the kinematics of the absorbers (as revealed by their unsaturated, low ionization metal line profiles) showed that these profiles are asymmetric in most DLAS. The asymmetries can be simply interpreted if the absorption arises in a thick, rapidly rotating disk (Prochaska & Wolfe 1997, Prochaska & Wolfe 1998), consistent with the idea that the absorbers are the progenitors of massive spiral galaxies. However, it has been shown that the observed line profiles can also be explained by mergers of sub-galactic clumps in hierarchical clustering scenarios (Haehnelt et al. 1998), by dwarf galaxy ejecta (Nulsen et al. 1998) and even by randomly moving clouds in a spherical halo (McDonald & Miralda-Escude 1999). Further, Ledoux et al. (1998) found that the asymmetry of the metal line profiles is pronounced only for systems with $\Delta V < 150 \text{ km s}^{-1}$; this is contrary to what would be expected if DLAS were indeed massive rotating disks (see, however, Wolfe & Prochaska 1998).

DLAS are known to contain some dust (Pei, Fall & McMahan 1989) and the problems of quantitatively accounting for dust depletion make the study of their metallicities and chemical evolution difficult. Studies using the abundances of metals like S or Zn, which are only slightly depleted onto dust grains (Pettini et al. 1997, Pettini et al. 1999), as well as attempts at modelling dust depletion (Vladilo 1998), indicate that the absorbers have low metallicities ($Z \lesssim 0.1Z_{\odot}$) and do not show much metallicity evolution with redshift. Further, DLAS do not show the $[\alpha/\text{Fe}]$ enrichment pattern that characterizes low metallicity halo stars in the Milky Way (Pettini et al. 1999, Molaro et al. 1998, Centurión et al. 2000). This difference in the $[\alpha/\text{Fe}]$ enrichment pattern suggests that DLAS have star formation histories different from spirals and more like those of dwarf galaxies.

Send offprint requests to: Nissim Kanekar

* nissim@ncra.tifr.res.in

** chengalur@ncra.tifr.res.in

In the local universe, the overwhelming contribution to the cross section for DLA absorption is believed to be made by the disks of spiral galaxies (Rao & Briggs 1993, Rao & Turnshek 1998); one might then expect at least the low redshift DLAS to be associated with spiral disks. Hubble Space Telescope (HST) and ground-based imaging have, however, shown that low z DLAS are, in fact, associated with a wide variety of morphological types (Le Brun et al. 1997, Rao & Turnshek 1998, Turnshek et al. 2000) and are not exclusively (or even predominantly) large spirals.

If the QSO behind the absorbing system is radio-loud, 21 cm absorption observations can be used to probe physical conditions and kinematics in the absorbers (see, for example, Chengalur & Kanekar 2000, Lane et al. 2000, Carilli et al. 1996). Such studies directly yield the spin temperature of the absorbing gas, which, for a homogeneous absorber, is typically the same as its kinetic temperature (Field 1958). For a multi-phase absorber, the measured spin temperature is the column density weighted harmonic mean of the temperatures of the individual phases.

Chengalur & Kanekar (2000) found that low T_s values ($T_s \lesssim 300$ K) were obtained in the few cases where the absorber was identified to be a spiral galaxy. Such temperatures are typical of the Milky Way and local spirals (Braun & Walterbos 1992, Braun 1997). However, the majority of DLAS have far higher spin temperatures, $T_s > 500$ K (Carilli et al. 1996, Chengalur & Kanekar 2000). Higher T_s values are to be expected in smaller systems like dwarf galaxies, whose low metallicities and pressures are not conducive to the formation of the cold phase of HI (Wolfire et al. 1995); such systems hence have a higher fraction of warm gas as compared to normal spirals, and therefore, a high spin temperature. Thus, the 21 cm absorption data appear to indicate that the majority of damped systems arise in dwarf or LSB galaxies, with only a few systems (at low redshifts) being luminous disks. Further, deep searches for HI emission from two of these high T_s objects have resulted in non-detections (Kanekar et al. 2000a, Lane et al. 2001), ruling out the possibility that they are under-luminous but gas-rich galaxies.

The Chengalur & Kanekar (2000) compilation of DLAS with published 21 cm absorption studies has only eighteen systems. We report, in this paper, on Giant Metrewave Radio Telescope (GMRT) 21 cm observations of three new candidate and confirmed damped absorbers at low redshift. Absorption was detected in two cases, while, for the third system, the non-detection imposes a high lower limit on the spin temperature. The rest of this paper is divided as follows : Sect. 2 describes the GMRT observations. Sect. 3 discusses the derivation of the spin temperatures from our 21 cm observations and also the properties of 21 cm absorbers in general. All dis-

tance dependent quantities in this paper are quoted for $H_0 = 75 \text{ km s}^{-1} \text{ Mpc}^{-1}$ and $q_0 = 0.5$.

2. Observations and Data analysis

The observations were carried out using the GMRT between February and April 2000. A 30-station FX correlator, which gives a fixed number of 128 channels over a bandwidth which can be varied between 64 kHz and 16 MHz, was used as the backend. The number of antennas used varied between ten and twelve owing to various debugging and maintenance activities; the longest baseline was ~ 1 km. Observational details are summarised in Table 1; note that the resolution listed is the channel spacing, i.e. before Hanning smoothing, while the RMS noise is over the smoothed spectrum. We discuss the individual sources below, in order of increasing redshift.

PKS 0952+179, $z_{\text{abs}} = 0.2378$: GMRT observations of PKS 0952+179 were carried out on three occasions, on the 28th of February, and the 3rd and 16th of April, 2000. A bandwidth of 2 MHz was used on the first of these dates and of 1 MHz on the other two (i.e. channel spacings of $\sim 4 \text{ km s}^{-1}$ and 2 km s^{-1} respectively). The total on-source time was 5 hours for the 1 MHz bandwidth observations. 0839+187 was used for phase calibration and observed every forty minutes in each run; 3C48 and 3C147 were used for absolute flux and bandpass calibration.

B2 0827+243, $z_{\text{abs}} = 0.5247$: This source was observed twice, on the 27th of March and the 10th of April, 2000, with a bandwidth of 2 MHz (channel spacing $\sim 5 \text{ km s}^{-1}$). The total on-source time was three hours in each case. 0851+202 was used as the phase calibrator while 3C48 and 3C295 were used to calibrate the system bandpass.

PKS 0118-272, $z_{\text{abs}} = 0.5579$: PKS 0118-272 was observed on the 9th of April, 2000, using a bandwidth of 2 MHz (channel spacing $\sim 5 \text{ km s}^{-1}$). 0114-211 was used as the phase and bandpass calibrator. Bandpass calibration was also carried out using 3C48 and 3C147. The total on-source time was four hours.

The data were analysed in AIPS using standard procedures. All three target sources were unresolved by the GMRT synthesised beam and there was no extended emission present in any of the fields. In the case of B2 0827+243 and PKS 0118-272, the field contained a few weak compact sources, but quite far from the phase centre; the analysis was hence quite straightforward. Continuum emission was subtracted by fitting a linear polynomial to the U-V visibilities, using the AIPS task UVLIN. The continuum-subtracted data were then mapped in all channels and spectra extracted at the quasar location from the resulting three-dimensional data cube. Spectra were also extracted at other locations in the cube to ensure that the data were not corrupted by interference. In case of multi-epoch observations of a single source, the spectra were corrected to the heliocentric frame outside AIPS and then averaged together.

Table 1. Observational details

Source	z_{abs}	N_{HI} cm^{-2}	Channel spacing* km s^{-1}	Total flux Jy	RMS noise mJy	τ	f^\dagger	T_s K
PKS 0952+179	0.2378	$2.1 \times 10^{21}{}^a$	2.0	1.4	2.9	0.013	0.25	2050 ± 200
B2 0827+243	0.5247	$2.0 \times 10^{20}{}^a$	5.0	0.9	1.2	0.0067	0.66	330 ± 70
PKS 0118-272	0.5579	$2.0 \times 10^{20}{}^b$	5.0	1.1	2.4	$< 0.0065^\ddagger$	0.5	$> 850^\ddagger$

* The RMS values are *after* Hanning smoothing.

† The values quoted are lower limits on the covering factor f .

‡ Limits are 3σ .

^a Rao & Turnshek (2000), ^b Vladilo et al. (1997)

Fig. 1 shows the 1 MHz GMRT spectrum of the absorber towards PKS 0952+179. The spectrum has been Hanning smoothed and has an RMS noise level of ~ 2.9 mJy per 4 km s^{-1} resolution element. Absorption was detected on all three observing runs, with the correct Doppler shift. The measured quasar flux is 1.4 Jy; the peak line depth is ~ 18.8 mJy and occurs at a heliocentric frequency of 1147.522 MHz, i.e. $z = 0.23780 \pm 0.00002$. The peak optical depth is ~ 0.013 .

The final Hanning smoothed spectrum of the $z = 0.5247$ absorber towards B2 0827+243 is shown in Fig. 2; the resolution is $\sim 10 \text{ km s}^{-1}$. The RMS noise on the spectrum is 1.15 mJy while the peak line depth is ~ 6 mJy, i.e. a 5.2σ result. The measured line depth is consistent with the reported non-detection by Briggs & Wolfe (1983); their 3σ upper limit on the line depth was ~ 7 mJy. We note that the absorption was again seen on both observing runs; however, the Doppler shift between the two epochs was slightly less than a channel and hence cannot be used as a test for the reality of the feature. No evidence for interference was seen in the data, on either the source or the calibrators. The absorption is quite wide, with a full width between nulls of $\sim 50 \text{ km s}^{-1}$, and a peak optical depth of ~ 0.0067 , at a frequency of 931.562 MHz, i.e. $z = 0.52476 \pm 0.00005$.

Finally, no absorption was detected in the $z = 0.5579$ absorber towards PKS 0118-272. The RMS noise on the final Hanning smoothed spectrum (resolution $\sim 10 \text{ km s}^{-1}$; not shown here) is ~ 2.4 mJy; this yields a 3σ upper limit of $\tau < 0.0065$ on the optical depth of the absorber.

3. Discussion

3.1. The spin temperature

The 21 cm optical depth, τ_{21} , of an optically thin, homogeneous cloud is related to the column density of the absorbing gas N_{HI} and the spin temperature T_s by the expression (e.g. Rohlfs 1986)

$$N_{\text{HI}} = \frac{1.823 \times 10^{18} T_s}{f} \int \tau_{21} dV, \quad (1)$$

where f is the covering factor of the absorber. In the above equation, N_{HI} is in cm^{-2} , T_s in K and dV in km s^{-1} . For

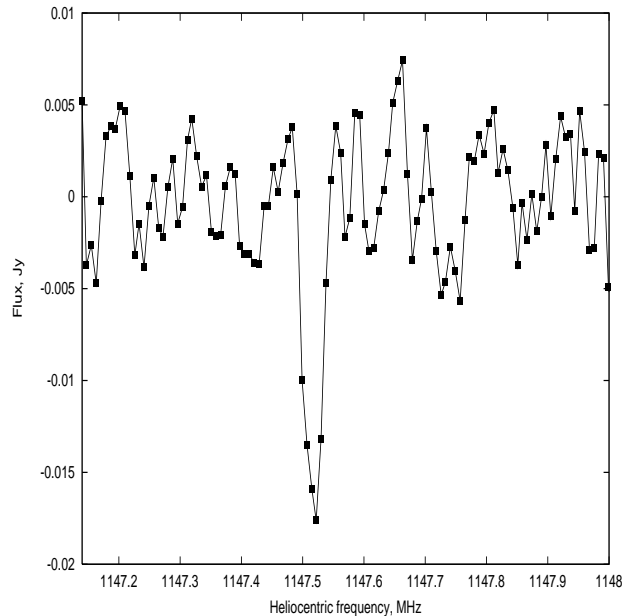


Fig. 1. GMRT HI spectrum towards PKS 0952+179. The x -axis is heliocentric frequency, in MHz. The spectrum has been Hanning smoothed and has a resolution of $\sim 4 \text{ km s}^{-1}$.

a multi-phase absorber the spin temperature derived using the above expression is the column density weighted harmonic mean of the spin temperatures of the individual phases. In the case of damped systems, the column density can be estimated from the equivalent width of the Lyman- α profile; a measurement of τ_{21} then yields the spin temperature *if* the covering factor is known. The latter is frequently uncertain since the radio emission from quasars is often extended while the UV continuum arises essentially from a point source. Thus, the line of sight along which the HI column density has been estimated need not be the same as the one for which the 21 cm optical depth has been measured. VLBI observations, when available, can be used to estimate the amount of radio emission emanating from compact components spatially coincident with the UV point source; one can then estimate f and thus, the spin temperature.

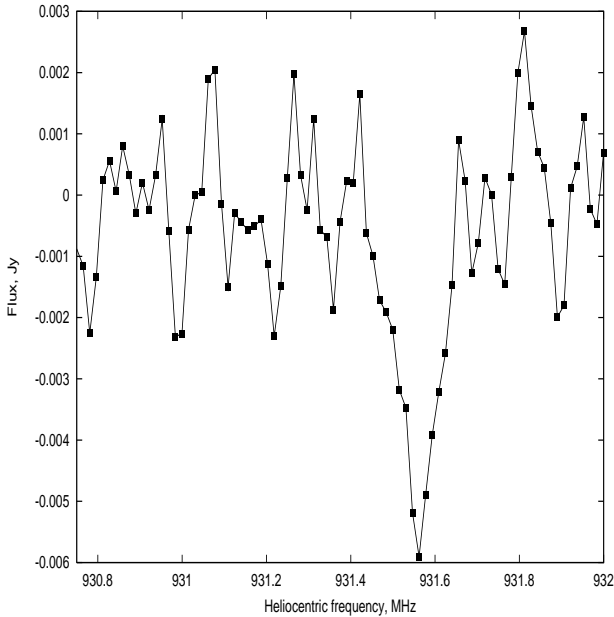


Fig. 2. GMRT HI spectrum towards B2 0827+243. The x -axis is heliocentric frequency, in MHz. The spectrum has been Hanning smoothed and has a resolution of $\sim 10 \text{ km s}^{-1}$.

PKS 0952+179 is a calibrator for the VLA A array, with a flux of 1.1 Jy at 1.4 GHz (resolution $\sim 1''$), besides some weak extended emission. 2.3 GHz VLBA observations (see the Radio Reference Frame Image Database of the United States Naval Observatory, henceforth RRFID) have resolved this core into a central component and some extended structure, with the entire emission contained within ~ 40 milli-arcseconds. Of these, the central component has a flux of ~ 370 mJy at 2.3 GHz, within ~ 20 milli-arcseconds; this component was further resolved by VLBA observations at 8.3 GHz (RRFID) into three components, all within ~ 15 milli-arcseconds. The total emission from these three components is similar to the flux of the central component at 2.3 GHz, implying that the region has a fairly flat spectrum. If one assumes that the spectrum of this region remains flat down to the frequency of our 21 cm observations (~ 1147.5 MHz) then the small size (~ 48 pc at $z = 0.2378$) implies that the absorber is likely to cover *at least* 370 mJy of the total quasar flux. Since the total flux measured by our GMRT observations is 1.4 Jy, the lower limit to the covering factor is $f_{\text{min}} \sim 0.25$. The column density derived from our observations is then $1.02 \pm 0.15 \times 10^{18} \text{ T}_s (0.25/f) \text{ cm}^{-2}$. HST observations of the Lyman- α line (Rao & Turnshek 2000) give $N_{\text{HI}} = 2.1 \times 10^{21} \text{ cm}^{-2}$, comparing this to our 21 cm estimate yields a spin temperature $T_s = 2050(f/0.25) \pm 200$ K. (Note that T_s would be higher if a larger amount of source flux was covered by the absorber and vice-versa.) The best-fit Gaussian to the GMRT spectrum of Fig. 1 has an FWHM $\sim 7.7 \text{ km s}^{-1}$. If one assumes that this width

is entirely due to thermal motions, one obtains a kinetic temperature $T_k \sim 1500$ K, lower than (but, given the error bars, not very different from) our estimate of the spin temperature. Note that standard models of the structure of the galactic ISM (see Kulkarni & Heiles (1988) for a review) do not permit a stable phase with a kinetic temperature of 1500 K; a detailed analysis of heating and cooling mechanisms in the neutral ISM (Wolfire et al. 1995) found two stable phases (the CNM and WNM), with temperatures in the range 41 - 200 K and 5500 - 8700 K respectively (with these values decreasing slightly with a decrease in the metallicity).

In the case of B2 0827+243, the optical quasar spectrum shows strong MgII absorption at $z = 0.5247$ (Ulrich & Owen 1977). HST observations (Rao & Turnshek 2000) found the Lyman- α line to be damped, but measure a slightly different redshift, viz. $z = 0.518$, with $N_{\text{HI}} = 2.0 \times 10^{20} \text{ cm}^{-2}$. No obvious explanation exists for the above discrepancy in redshift, except for a possible error in the wavelength calibration of one of the observations. The GMRT spectrum of Fig. 2 shows 21 cm absorption centred at a redshift of $z = 0.52476$, in agreement with the MgII redshift of Ulrich & Owen (1977); this indicates that the HST observations may have had an error in the wavelength correction.

VLA 20 cm A array observations of B2 0827+243 obtained a flux density of 550 mJy in an unresolved core component (size $< 1''$) (Price et al. 1993). This component was found to remain unresolved in subsequent VLBA observations at 2.3 GHz and 8.5 GHz (resolution $\simeq 20$ milli-arcseconds, this corresponds to a linear size of 100 pc at $z = 0.5247$) with a flux of ~ 600 mJy at both frequencies (RRFID). Our GMRT observations measured a flux of ~ 900 mJy at 931 MHz (in good agreement with the 931 MHz flux quoted by Briggs & Wolfe (1983)); if the core contains at least 600 mJy and is completely covered, one obtains $f \gtrsim 0.66$. The column density of the absorbing gas is thus $N_{\text{HI}} = 6.1 \pm 1.1 \times 10^{18} \text{ T}_s (0.66/f) \text{ cm}^{-2}$, from our observations, implying a spin temperature $T_s = 330 (f/0.66) \pm 70$ K. Note that a covering factor of unity gives $T_s = 470$ K; this is the upper limit on the spin temperature.

The $z = 0.5579$ absorber towards PKS 0118-272 is a candidate damped system, for which Vladilo et al. (1997) estimate $N_{\text{HI}} \sim 2 \times 10^{20} \text{ cm}^{-2}$. This column density is, however, estimated from low-ionization metal lines and *not* from observations of the Lyman- α transition (see also Rao & Turnshek (2000)). VLBI observations of the quasar at 5 GHz (Shen et al. 1998) measured a flux of 550 mJy within the central 20 milli-arcseconds (corresponding to a linear size of 100 pc at $z = 0.5579$). Further, a single-baseline 2.3 GHz VLBI observation yielded a flux of 530 ± 0.05 mJy (Preston et al. 1985). The flatness of the core spectrum implies that it is reasonable to expect the core to contain ~ 550 mJy of flux at 911 MHz, our observing frequency. Our GMRT observations measured a flux of \sim

1.1 Jy; the lower limit to the covering factor is thus ~ 0.5 . The RMS noise of ~ 2.4 mJy (per 10 km s $^{-1}$ channel) then gives a 3σ lower limit of $850(f/0.5)$ K on the spin temperature.

Deep K-band imaging and spectroscopy of the B2 0827+243 field (Turnshek et al. 2000) have identified a spiral galaxy at $z = 0.524$ as the system giving rise to the damped absorption. The low estimated spin temperature of the absorber continues the trend noted earlier (Chengalur & Kanekar 2000) for DLAS associated with spirals to have low T_s . Interestingly, the impact parameter of the quasar line of sight to the absorbing galaxy is ~ 28 kpc (Turnshek et al. 2000); the low spin temperature then implies that substantial amounts of cold HI are present even at such large distances from the galaxy centre.

The field around PKS 0952+179 has also been imaged by Turnshek et al. (2000) in the K-band, and the absorber tentatively identified as an LSB galaxy. No large spiral is present in the field, consistent with the high spin temperature obtained for this system. For the candidate DLAS PKS 0118-272 Vladilo et al. (1997) find that the [Ti/Fe] and [Mn/Fe] ratios are similar to that of diffuse ISM clouds and identify by PSF subtraction a candidate absorbing galaxy at an impact parameter of 8 kpc; the redshift of this galaxy is however unknown. If the galaxy is at the same redshift as the absorption line system it would have $M_R \sim -21$.

3.2. Properties of 21 cm absorbers

The sample of DLAS with published 21 cm observation observations presently consists of 22 systems (the 18 absorbers listed in (Chengalur & Kanekar 2000), the three described here and the $z = 0.101$ candidate towards PKS 0439-433 (Kanekar et al. 2000a)). Fig. 3 shows a plot of spin temperature versus redshift, for 21 systems of the sample (the $z \sim 0.437$ absorber towards 3C196 is excluded since its N_{HI} is uncertain); it can be seen that the majority of DLAS have T_s values far higher than those of the Milky Way, with the only exceptions being systems identified as spiral galaxies. If damped systems have the same two-phase structure seen in our Galaxy, this would mean that the absorbers have higher amounts of the warm phase of neutral hydrogen (WNM) than normal spirals (Chengalur & Kanekar 2000). Fig. 4 plots the “true” 21 cm equivalent width (i.e. $EW = [\int \tau_{21} dV]/f$) of 21 systems of the sample (again excluding the $z = 0.437$ DLA towards 3C196) against HI column density, on a logarithmic scale; it can be seen that the trend for increasing EW with N_{HI} , seen in Galactic data (Carilli et al. 1996), persists for damped Lyman- α systems. More importantly, DLAS identified as spiral galaxies (open squares) can be seen to have systematically higher equivalent widths, at the same values of HI column density. Further, most DLAS (except the ones identified as spirals) tend to lie around

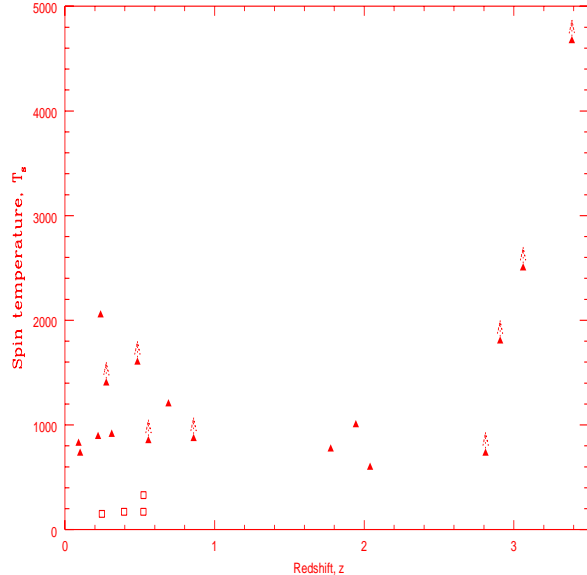


Fig. 3. The figure shows the spin temperature T_s plotted against redshift, for 21 DLAS, excluding the $z = 0.437$ absorber towards 3C196. DLAS identified as spiral galaxies are shown as hollow squares, while lower limits on the spin temperature are indicated by upward arrows.

the lower edge of the envelope defined by the Galactic data (see Carilli et al. (1996) for a comparison). This also indicates (as suggested earlier by Carilli et al. (1996)) that the majority of DLAS contain a higher fraction of the warm phase of neutral hydrogen than normal spirals like the Milky Way, and are hence unlikely to be spiral galaxies. Similarly, Petitjean et al. (2000)) used observations of molecular hydrogen in a sample of DLAS to conclude that most damped absorption arises in warm ($T > 3000$ K) gas.

Direct evidence for the proposition that damped systems have a larger WNM content as compared to local spirals comes from the high resolution Arecibo observations of the two DLAS towards OI363 (Lane et al. 2000, Kanekar et al. 2000b). In the case of the lower redshift ($z = 0.0912$) system, the ratio of column densities of the WNM to CNM is $\gtrsim 2:1$ (Lane et al. 2000), while, for the $z = 0.2212$ absorber, this ratio is $\gtrsim 3:1$ (Kanekar et al. 2000b). Thus, at least in these two systems, the WNM to CNM ratio is higher than that seen in spiral galaxies and is, in fact, similar to values obtained in dwarf systems (Young et al. 2000).

If the high spin temperatures of the majority of damped absorbers arise due to their lower metallicities and hence, larger fractions of the WNM (Chengalur & Kanekar 2000), one would expect that the metallicities (i.e. the [Zn/H] ratios) of the DLAS identified as spirals should be systematically higher than those of systems with high T_s values. Unfortunately, [Zn/H] estimates exist for only six DLAS of the sam-

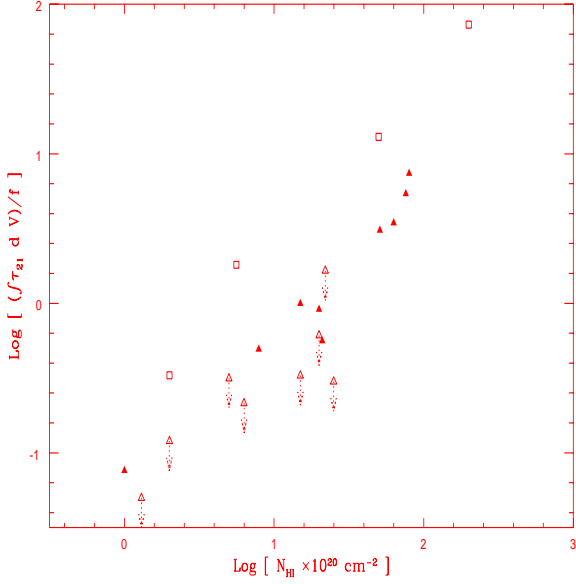


Fig. 4. The figure shows the “true” 21 cm equivalent width $EW = [\int \tau dv]/f$ plotted against HI column density N_{HI} , on a logarithmic scale. Spiral galaxies are indicated by hollow squares, while filled and open triangles indicate detections and non-detections of absorption, respectively, in the remaining systems.

ple and for only one low T_s system (the $z \sim 0.395$ absorber towards PKS 1229-021) (Boissé et al. 1998, Pettini et al. 1994, Pettini et al. 1997, Meyer et al. 1989, Meyer & York 1992). These values are plotted against spin temperature in Fig. 5; it can be seen that the low T_s system has the highest $[\text{Zn}/\text{H}]$ ratio of all six absorbers. It would be very interesting to test whether this trend persists, for the other absorbers in the sample.

Figs. 6 and 7 plot the velocity spread ΔV (full width between nulls) of the systems with detected 21 cm absorption against redshift and spin temperature, respectively. (The total velocity spread is used, instead of the FWHM of the absorption profile, to account for the possibility that a single line of sight intersects multiple clouds, as is typical in spiral galaxies.) The plot of ΔV versus redshift indicates that large velocity spreads ($\Delta V > 100 \text{ km s}^{-1}$) are not found for $z \gtrsim 2$, while both large and small spreads are seen at low redshift. Similarly, Fig. 3 shows that, while both low and high T_s values are obtained at low redshift, only high values are obtained for $z \gtrsim 1.5$. This is qualitatively consistent with what is expected in hierarchical clustering models (e.g. Kauffmann 1996), in which systems with low circular velocities dominate the absorption cross-section at high redshift, while systems with both high and low circular velocities are found at low z . Next, Fig. 7 shows a possible correlation between the velocity width and the spin temperature of the absorbers, with only one system (the $z = 0.3127$ absorber

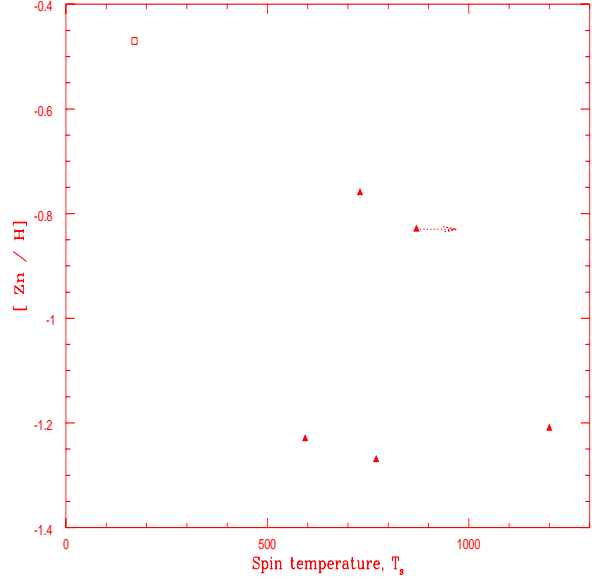


Fig. 5. The figure shows the $[\text{Zn}/\text{H}]$ ratio plotted against spin temperature T_s , for the six damped systems with $[\text{Zn}/\text{H}]$ estimates. The $z \sim 0.395$ absorber towards PKS 1229-021 is indicated by a hollow square.

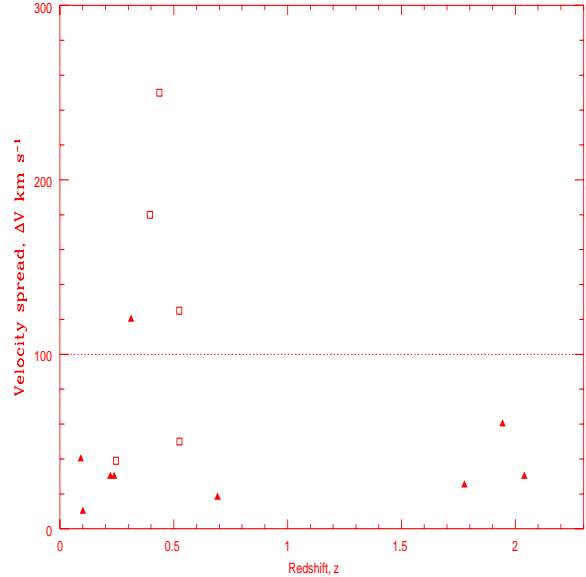


Fig. 6. The figure shows the 21 cm velocity spread ΔV plotted against redshift for all damped systems with detected 21 cm absorption. Absorbers identified as spiral galaxies are shown as hollow squares.

towards PKS 1127-145) having both a large 21 cm velocity spread and a high temperature; all other systems with large ($\Delta V > 100 \text{ km s}^{-1}$) velocity widths are identified with low T_s spirals. The system towards PKS 1127-145 is likely to be tidally disturbed since there are at least

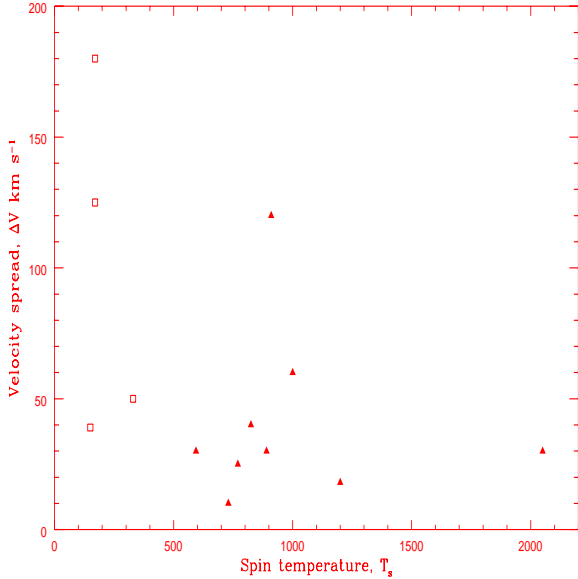


Fig. 7. The figure shows the 21 cm velocity spread ΔV plotted against spin temperature T_s , for all damped systems with detected 21 cm absorption. Absorbers identified as spiral galaxies are shown as hollow squares. Note that the $z = 0.437$ absorber towards 3C196 has not been included in the figure since its spin temperature is unknown; see discussion in text.

three galaxies at the redshift of the damped Lyman- α absorber (Lane et al. 1998). (Note also that the $z \sim 0.437$ absorber towards 3C196 has not been included in this figure, since its T_s is unknown. However, the observations are consistent with $T_s \lesssim 200$ K (de Bruyn et al. 2001), while the velocity spread is 250 km s^{-1} ; it would hence lie close to the upper left corner of the figure.) The average velocity spread for the absorbers identified as spirals is $\Delta V_{ave} \sim 130 \text{ km s}^{-1}$ while, for the high T_s systems, the mean spread is far lower, $\Delta V_{ave} \sim 40 \text{ km s}^{-1}$.

It should be emphasised that the results on the velocity widths of the absorption lines stem from the sub-sample of 14 systems which show 21 cm absorption; the statistics should clearly be improved before any strong conclusions can be drawn. However, although the numbers are small, the general trends in T_s and ΔV are consistent with scenarios in which damped Lyman- α absorbers are typically small systems at high redshift, while, at low redshift, they are a composite population including both spiral galaxies as well as smaller systems.

Acknowledgements. These observations would not have been possible without the many years of dedicated effort put in by the GMRT staff in order to build the telescope. This research has made use of the United States Naval Observatory (USNO) Radio Reference Frame Image Database (RRFID).

References

- Boissé P., le Brun V., Bergeron J., Deharveng, J.-M., 1998, *A&A*, 333, 841.
 Braun R., Walterbos R., 1992, *ApJ*, 386, 120.
 Braun R., 1997, *ApJ*, 484, 637.
 Carilli C. L., Lane W., de Bruyn A. G., Braun R., Miley G. K., 1996, *AJ*, 111, 1830.
 Briggs F. H., Wolfe A. M., *ApJ*, 268, 76.
 Centurión M., Bonifacio P., Molaro P., Vladilo G., 2000, *ApJ*, 536, 540.
 Chengalur J. N., Kanekar N., 1999, *MNRAS*, 302, L29.
 Chengalur J. N., Kanekar N., 2000, *MNRAS*, 318, 303.
 de Bruyn A. G., O’Dea C. P., Baum S. A., 1996, *A&A*, 305, 450.
 de Bruyn A. G., Briggs F. H., Vermuelen R., 2001, in preparation.
 Field G. B., 1958, *Proc. IRE*, 46, 240.
 Haehnelt M. G., Steinmetz M., Rauch M., 1998, *ApJ*, 495, 64.
 Kanekar N., Chengalur J. N., Subrahmanyam R., Petitjean P., 2000, accepted by *A&A*.
 Kanekar N. et al., 2000, in preparation.
 Kauffmann G., 1996, *MNRAS*, 281, 475.
 Kulkarni S. R. & Heiles C., 1988, in *Galactic and Extra-Galactic Radio Astronomy* (2nd edition), G. Verschuur & K. I. Kellermann eds., Springer-Verlag (Berlin and New York), 95.
 Le Brun V., Bergeron J., Boissé P., Deharveng J.-M., 1997, *A&A*, 321, 733.
 Lane W., Smette A., Briggs F. H., et al., 1998, *AJ*, 116, 26.
 Lane W., Briggs F. H., Smette A., 2000, *ApJ*, 532, 146.
 Lane W., Briggs F. H., Kanekar N., Chengalur J. N., 2001, in preparation.
 Lanzetta K. M., Wolfe A. M., Turnshek D. A., et al., 1991, *ApJS*, 77, 1.
 Lanzetta K. M., Wolfe A. M., Turnshek D. A., 1995, *ApJ*, 440, 435.
 McDonald P., Miralda-Escude J., 1999, *ApJ*, 519, 486.
 Meyer D. M., Welty D. E., York D. G., 1989, *ApJ*, 343, L37.
 Meyer D. M., York D. G., 1992, *ApJ*, 399, 121.
 Molaro P., Centurión M. Vladilo G., 1998, *MNRAS*, 293, L37.
 Nulsen P. E. J., Barcons X., Fabian A. C., 1998, *MNRAS*, 301, 168.
 Pei Y. C., Fall M. S., McMahon R. G., 1989 *ApJ*, 341, L5.
 Pettini M., Smith L. J., Hunstead R. W., King D. L., 1994, *ApJ*, 426, 79.
 Pettini M., King D. L., Smith L. J., Hunstead R. W., 1997, *ApJ*, 486, 665.
 Pettini M., Ellison, S. L., Steidel C. C., Bowen D. V., 1999, *ApJ* 510, 576.
 Preston R. A., Morabito D. D., Williams J. G., et al., 1985, *AJ*, 90, 1599.
 Price R., Gower A. C., Hutchings J. B., et al., 1993, *ApJS*, 86, 365.
 Prochaska J. X., Wolfe A. M., 1997, *ApJ*, 487, 73.
 Prochaska J. X., Wolfe A. M., 1998, *ApJ*, 507, 113.
 Rao S. M., Briggs F. H., 1993, *ApJ*, 419, 515.
 Rao S. M., Turnshek, D. A., 1998, *ApJ*, 500, L115.
 Rao S. M., Turnshek, D. A., 2000, *ApJS*, 130, 1.
 Rohlfs K., 1986, *Tools of Radio Astronomy*, (Springer-Verlag, Berlin Heidelberg)
 Shen Z.-Q. et al., 1998, *AJ*, 115, 1357.

- Petitjean P., Srianand R., Ledoux C., 2000, accepted by A&A Special issue (astro-ph:0011437).
- Turnshek D. A., Rao S. M., Lane W., Monier E., Nestor D., 2000, to appear in proceedings of the “Gas and Galaxy Evolution” conference, J. E. Hibbard, M. P. Rupen and J. H. van Gorkom eds. (astro-ph:0009096).
- Ulrich M. -H., Owen F. N., 1977, *Nature*, 269, 673.
- Vladilo G., 1998, *ApJ*, 493, 583.
- Vladilo G., Centurión M., Falomo R., Molaro P., 1997, *A&A*, 327, 47.
- Wolfe A. M., Turnshek D. A., Smith H. E., Cohen R. D., 1986, *ApJS*, 61, 249.
- Wolfe A. M., 1988, in *QSO Absorption Lines: Probing the Universe*, J. C. Blades et al. eds., Cambridge University Press.
- Wolfe A. M., Prochaska J. X., 1998, *ApJ*, 494, L15.
- Wolfire M. G., Hollenbach D., McKee C. F., Tielens A. G. G. M., Bakes E. L. O., 1995, *ApJ*, 443, 152.
- Young L. M., van Zee L., Dohm-Palmer R. C., Lo K. Y., 2000, to appear in proceedings of the conference “Gas and Galaxy Evolution”, J. E. Hibbard, M. P. Rupen and J. H. van Gorkom eds., (astro-ph:0009069).